Dynamical non-ergodic scaling in continuous finite-order quantum phase transitions

To cite this article: S. Deng *et al* 2008 *EPL* **84** 67008

View the article online for updates and enhancements.

Dynamical non-ergodic scaling in continuous finite-order quantum phase transitions

S. Deng[1], G. Ortiz[2] and L. Viola[1](a)

[1] *Department of Physics and Astronomy, Dartmouth College, 6127 Wilder Laboratory - Hanover, NH 03755, USA*
[2] *Department of Physics, Indiana University - Bloomington, IN 47405, USA*

Abstract – We investigate the emergence of universal dynamical scaling in quantum critical spin systems adiabatically driven out of equilibrium, with emphasis on quench dynamics which involves non-isolated critical points (*i.e.*, critical regions) and cannot be *a priori* described through standard scaling arguments nor time-dependent perturbative approaches. Comparing to the case of an isolated quantum critical point, we find that non-equilibrium scaling behavior of a large class of physical observables may still be explained in terms of equilibrium critical exponents. However, the latter are in general non-trivially path-dependent, and detailed knowledge about the time-dependent excitation process becomes essential. In particular, we show how multiple level crossings within a gapless phase may completely suppress excitation depending on the control path. Our results typify non-ergodic scaling in continuous finite-order quantum phase transitions.

The response of a physical system to external probes is an invaluable technique for unveiling the system's properties. If the probe is dynamic, so that the Hamiltonian becomes explicitly time-dependent, the system is forced out of equilibrium – a subject of prime practical importance which can soon prove full of challenges and surprises. In particular, understanding and manipulating the dynamics of zero-temperature quantum phase transitions (QPTs) [1] in matter has a broad significance across fields as diverse as quantum-statistical mechanics, material science, quantum information processing, and cosmology. The extent to which universal quantum scaling laws persist out of equilibrium and encode information about the equilibrium phase diagram is the topic of this work.

As early as 1970, Barouch and coworkers [2] studied the time-dependent $T = 0$ magnetization of the anisotropic XY chain, and showed that equilibrium is not reached at the final evolution time. This *non-ergodic* behavior was later confirmed for other physical observables [3], and the analysis extended to the case where the system is driven across its quantum critical point (QCP) by changing a control parameter $\lambda(t)$ (*e.g.*, the magnetic field along the z-axis) in time with constant quench rate $\tau > 0$.

The emergence of non-equilibrium scaling, however, was not discussed. An important step was taken in ref. [4], starting from the observation that irrespective of how slowly the quench occurs, adiabaticity is lost in the thermodynamic limit at a "freeze-out" time $(t_c - \hat{t})$ before the QCP is crossed. This yields a power-law prediction for the final density of excitations, $n_{\mathrm{ex}}(t_{\mathrm{fin}}) \sim \xi^{-1}(\hat{t}) \sim \tau^{-\ell}$, where the *non-equilibrium critical exponent* $\ell = d\nu/(\nu z + 1)$ is solely determined by the equilibrium correlation length (ξ) the dynamic critical exponents of the QCP (ν and z, respectively), and the spatial dimension, d. While it is suggestive to realize that defect formation is a manifestation of broken ergodicity in Barouch's sense [3], continuous experimental advances in systems ranging from ultracold atomic gases to quantum magnets [5] demand the applicability of the above *Kibble-Zurek scaling* (KZS) to be carefully scrutinized, and the potential for more general *non-ergodic* scaling to be explored. How much information on the equilibrium physics is needed for reliable scaling predictions to be possible?

The KZS for linear quenches across an *isolated* QCP separating two gapped phases has been confirmed by now for a variety of control schemes in one-dimensional (1D) models [6–8], including QCPs of topological nature [9] and noisy driving fields [10] – generalizations to repeated [11]

(a)E-mail: Lorenza.Viola@Dartmouth.EDU

and non-linear quenches [12,13] having also been established. Leaving aside the case of *disordered* quantum systems, where marked deviations from power law behavior may be witnessed [14], the possibility of genuinely *non-adiabatic* scaling in low-dimensional clean systems, whereby non-zero excitation persists (unlike KZS) for $\tau \to \infty$ in the thermodynamic limit, has been pointed out in [8]. Likewise, critical dynamics in the presence of *non-isolated* QCPs reveals a rich landscape. The need to modify the KZS by replacing d with the "co-dimension" m of the relevant critical (gapless) surface has emerged through a study of the 2D Kitaev model [15]. Evidence of non-KZS has also been reported for quenches which originate within an extended quantum critical region [16], cross a multi-critical point [13,17], or steer the system along a gapless critical line [18].

A main purpose of this work is to develop a theory and understanding of non-ergodic scaling for generic (power law) quenches along critical regions. To achieve this goal two new notions are introduced, which are both *path-dependent*: one is the concept of a *dominant critical point* to establish scaling along a critical path, and the other a *mechanism of cancellation* of excitations. Besides elucidating several results recently reported in the literature, our analysis indicates that details on how different modes of excitation are accessed throughout the quench process are crucial. We consider several different scenarios within a unifying illustrative testbed, the 1D anisotropic XY model in a transverse alternating magnetic field [19]. In particular, we push beyond the KZS domain – notably, by investigating quenches that involve a continuous Lifshitz QPT to a gapless phase. We also revisit the standard KZS and clarify how, for arbitrary continuous QPTs, it can be accounted for by the *iterative adiabatic renormalization* approach of Berry [20], as long as two gapped quantum phases are involved. Most importantly, we find that universal dynamical scaling is obeyed by a large class of extensive physical observables *throughout the quench dynamics*, a result with practical implications in the experimental detection of non-ergodic scaling.

Model Hamiltonian. – The spin-1/2 anisotropic XY model in a transverse alternating field is defined by [19]

$$H = -\sum_{i=1}^{N} \left\{ \frac{1+\gamma}{2} \sigma_x^i \sigma_x^{i+1} + \frac{1-\gamma}{2} \sigma_y^i \sigma_y^{i+1} - [h - (-)^i \delta] \sigma_z^i \right\},$$
(1)

where periodic boundary conditions are assumed, that is, $\sigma_\alpha^i \equiv \sigma_\alpha^{i+N}$. Here, $\gamma \in [0, 1]$, $h, \delta \in [-\infty, \infty]$, are the anisotropy in the XY plane, and the uniform and alternating magnetic field strength, respectively. This model can be exactly solved by following the steps outlined in [19,21]. The Hamiltonian (1) rewrites as $H = \sum_{k \in K_+} \hat{H}_k = \sum_{k \in K_+} A_k^\dagger H_k A_k$, where $K_+ = \{\pi/N, 3\pi/N, \ldots, \pi/2 - \pi/N\}$ specifies allowed momentum values, and $A_k^\dagger = (a_k^\dagger, a_{-k}, b_k^\dagger, b_{-k})$ is a vector operator, with $a_k^\dagger$ ($b_k^\dagger$) denoting canonical fermionic
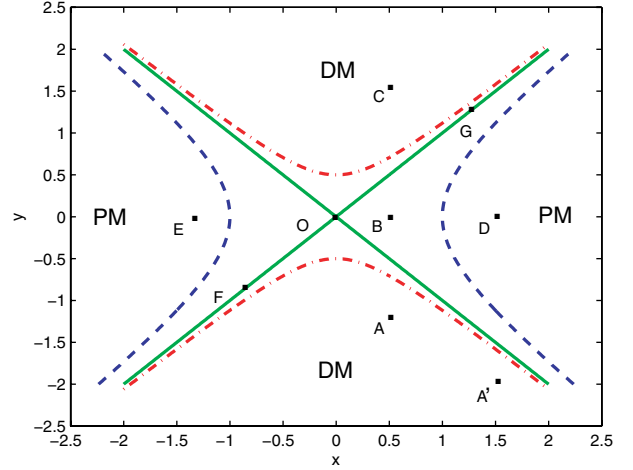

Fig. 1: (Colour on-line) Phase diagram of the alternating spin chain, eq. (1). Dashed (blue) and dashed-dotted (red) lines define the phase boundaries for $\gamma = 0.5$, the enclosed area corresponding to the FM phase. Dashed (blue) and solid (green) lines correspond to $\gamma = 0$, the enclosed area being the SF gapless phase.

operators that create a spinless fermion with momentum k for even (odd) sites. Diagonalization of the reduced 4×4 Hamiltonian matrix H_k further yields a collection of non-interacting quasi-particles,

$$H = \sum_{k \in K_+}^{n=1,\ldots,4} \epsilon_{k,n} N_{k,n},$$

in terms of an appropriate number operator $N_{k,n}$ for mode (k, n). Assuming that n labels bands in increasing energy order, only $\epsilon_{k,1}, \epsilon_{k,2} \leqslant 0$ bands are occupied at $T = 0$, with an excitation gap $\Delta_k = \epsilon_{k,3} - \epsilon_{k,2}$ being given by

$$\Delta_k(\gamma, h, \delta) = 4 \Big[h^2 + \delta^2 + \cos^2 k + \gamma^2 \sin^2 k$$
$$- 2\sqrt{h^2 \cos^2 k + \delta^2 (h^2 + \gamma^2 \sin^2 k)} \Big]^{1/2}. \quad (2)$$

Quantum phase boundaries are determined by the equations $h^2 = \delta^2 + 1$; $\delta^2 = h^2 + \gamma^2$. The phase diagram with both $\gamma = 0.5$ and $\gamma = 0$ is shown in fig. 1. Quantum phases corresponding to disordered paramagnetic (PM) and dimer (DM) behavior emerge as depicted for arbitrary γ. For $\gamma > 0$, ferromagnetic order (FM phase) develops in the center of the phase diagram, whereas for the isotropic chain a superfluid (SF) phase with a gapless spectrum and non-broken $U(1)$-symmetry emerges. Finite-size analysis reveals that this model supports four distinct universality classes: i) When $\gamma > 0$, generic QCPs belong to the $d = 2$ Ising universality class with critical exponents $\nu = 1, z = 1$. Different critical behavior occurs at $(h \to 0, \delta = \pm \gamma)$ and $(h = \pm 1, \delta \to 0)$, where weak singularities in the ground-state energy develop (4th-order QCPs [19]), and $\nu = 2, z = 1$, corresponding to the alternating universality class. ii) When $\gamma = 0$, generic QCPs on the boundary

lines belong to the Lifshitz universality class, with critical exponents $\nu = 1/2, z = 2$. Different critical behavior still occurs at $(h = \pm 1, \delta \to 0)$, where now $\nu = 1, z = 2$. Furthermore, Ising critical exponents are recovered while approaching the point $(h = 0, \delta = 0) \equiv O$ along every path other than $(\delta = 0, h \to 0)$ (when there is no QCP). In what follows, we focus on quenching schemes where h and δ are individually or simultaneously varied with time. We address separately different representative scenarios.

Quenching across an isolated critical point. – Suppose first that the system is *linearly* quenched across an isolated (non-multicritical) QCP that separates two gapped phases upon changing a single control parameter as $\delta\lambda(t) = \lambda(t) - \lambda_c = (t - t_c)/\tau$, where $t \in [t_{\rm in}, t_{\rm fin}]$. Without loss of generality we may assume that the system becomes critical at $t_c = 0$. For finite N, the exact time-evolved many-body state $|\psi(t)\rangle$ may be determined from numerical integration of the Schrödinger equation with Hamiltonian $H(t)$, subject to $|\psi(t_{\rm in})\rangle = |\psi_{GS}(t_{\rm in})\rangle$, the latter being the ground state of $H(t_{\rm in})$. The final excitation density $n_{\rm ex}(t_{\rm fin})$ may then be computed from the expectation value of the instantaneous quasi-particle number operator over $|\psi(t)\rangle$. Provided that the quench rate τ belongs to the appropriate range[1], KZS is found to hold irrespective of the details of the QCP and the initial (final) quantum phase, in particular for both 2nd- and higher-order QPTs, and independent of the path direction:

$$n_{\rm ex}^{\rm Ising}(t_{\rm fin}) \sim \tau^{-1/2}, \quad n_{\rm ex}^{\rm Alternating}(t_{\rm fin}) \sim \tau^{-2/3}.$$

While the excitation density is an accurate measure of the loss of adiabaticity in exactly solvable models, identifying manifestations of the KZS in quantities that can be more directly accessible in experiments and/or meaningful in more general systems is essential. Remarkably, numerical results indicate that scaling behavior holds throughout the quench process for a large class of physical observables, provided that the excess expectation value relative to the instantaneous ground state is considered [19]. That is

$$\Delta\mathcal{O}(t) \equiv \langle\psi(t)|\,\mathcal{O}\,|\psi(t)\rangle - \langle\psi_{GS}(t)|\,\mathcal{O}\,|\psi_{GS}(t)\rangle$$
$$= \tau^{-(\nu+\beta)/(\nu z+1)} F_{\mathcal{O}}\left(\frac{t-t_c}{\hat{t}}\right), \quad (3)$$

where β is a scaling exponent determined by the physical dimension of $\mathcal{O}$ and F is an observable-dependent scaling function. For instance, under a quench of the magnetic field strength, h, the magnetization per site, $M_z = (\sum_{i=1}^{N} \sigma_z^i)/N$, obeys dynamical scaling of the form $\Delta M_z(t) = \tau^{(-\nu-\nu z+1)/(\nu z+1)} G((t-t_c)/\hat{t})$, whereas the
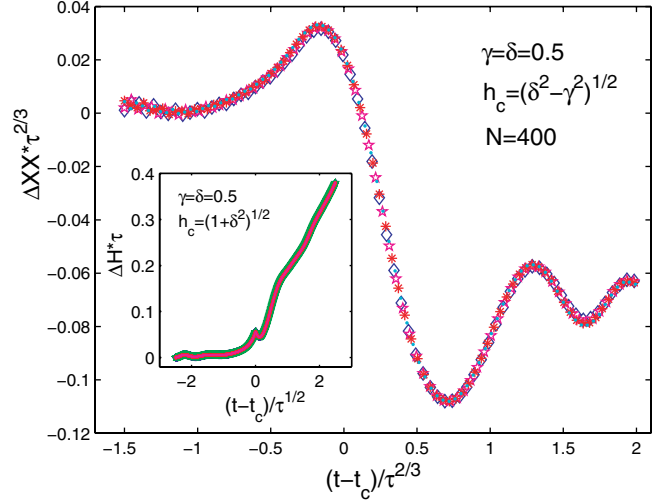

Fig. 2: (Colour on-line) Dynamical scaling under a magnetic field quench. Main panel: excess nearest-neighbor spin correlation per particle, ΔXX, *vs.* rescaled time for the alternating universality class from numerical integration of the Schrödinger equation. Inset: excess energy per particle, ΔH, *vs.* rescaled time for the Ising universality class from first-order adiabatic renormalization.

nearest-neighbor spin correlator along the x-direction, $XX = (\sum_{i=1}^{N} \sigma_x^i \sigma_x^{i+1})/N$, obeys dynamical scaling of the form $\Delta XX(t) = \tau^{-\nu/(\nu z+1)} W((t-t_c)/\hat{t})$, for appropriate scaling functions G and W, respectively – see fig. 2.

The fact that the system becomes gapless at a single instant t_c suggests to seek an explanation of the above results based on the fact that $\dot{\lambda}(t) = 1/\tau$ is a small parameter. While a similar strategy has been implemented in [8], our emphasis is on providing a firm theoretical foundation and further highlighting important assumptions. By a suitable parametrization, the relevant time-dependent Hamiltonian may be written as $H(t) = H_c + [\lambda(t) - \lambda_c]H_1 = H_c + (t-t_c)/\tau H_1$, with H_c quantum-critical in the thermodynamic limit. Let $\{E_m(t)\}$ and $\{|\psi_m(t)\rangle\}$ denote the snapshot eigenvalues and (orthonormal) eigenvectors of $H(t)$, where $|\psi_0(t)\rangle \equiv |\psi_{GS}(t)\rangle$ and assume that: i) no level crossing occurs throughout the evolution; ii) the derivatives of all the spectral projectors $\{|\psi_m(t)\rangle\langle\psi_m(t)|\}$ are sufficiently smooth. The (normalized) time-evolved state reads

$$|\psi(t)\rangle = c_0(t)|\psi_0(t)\rangle + \sum_{m\neq 0} c_m(t)|\psi_m(t)\rangle,$$

for coefficients to be determined. Since for a truly adiabatic evolution no excitation is induced in spite of the fact that the eigenstates of $H(t)$ evolve in time, appropriately subtracting (following Berry, "renormalizing") the adiabatic contribution is essential for quantifying the leading non-adiabatic correction. This is achieved in two steps [22]: i) effect a canonical transformation to a "comoving frame," where in the zeroth-order adiabatic limit $\tau \to \infty$ the comoving state vector $|\tilde{\psi}(t)\rangle = \tilde{U}(t;t_{\rm in})|\psi(t_{\rm in})\rangle$ is frozen up

---

[1]That $\tau \geqslant \tau_{\rm min}$ follows from standard adiabaticity requirements away from criticality, $\tau_{\rm min} \sim 1/[\min_{t \in [t_{\rm in}, t_{\rm fin}]}{\rm Gap}(H(t))]^2$. The existence of a finite upper bound $\tau_{\rm max}$ follows from the fact that if τ is arbitrarily large, a *finite* system never enters the impulsive regime, if the size-dependent contribution to the gap dominates over the control-dependent one. From scaling analysis under the assumption that the gap closes polynomially as N^{-z}, we estimate $\tau_{\rm max} \sim N^{(\nu z+1)/\nu}$.

to a phase factor, that is, $|\tilde{\psi}(t)\rangle = e^{-i\Gamma_0(t)}|\psi_0(t_{\text{in}})\rangle$, where $\Gamma_0(t)$ includes in general both the Berry phase and the dynamical phase; ii) evaluate the first-order correction to the comoving-frame propagator via Dyson series expansion. Transforming back to the physical frame, $c_m(t) = \langle\psi_m(t_{\text{in}})|\tilde{U}(t; t_{\text{in}})|\psi_0(t_{\text{in}})\rangle$, to first order in $\dot{\lambda}$ we finally obtain (in units $\hbar = 1$), $c_0^{(1)}(t) = e^{-i\Gamma_0(t)} + O(\dot{\lambda}^2)$, and

$$c_m^{(1)}(t) = e^{-i\Gamma_m(t)}\int_{t_{\text{in}}}^t \mathrm{d}t'\, \dot{\lambda}(t') \frac{\langle\psi_m(t')|H_1|\psi_0(t')\rangle}{E_m(t') - E_0(t')} e^{i\int_{t_{\text{in}}}^{t'}\mathrm{d}s\,\Delta_m(s)},$$
$$\Delta_m(t) = E_m(t) - E_0(t). \qquad (4)$$

Knowledge of the time-dependent state enables arbitrary physical quantities of interest to be computed, in particular the total time-dependent excitation probability $\mathbb{P}_{\text{ex}}(t) = \sum_{m\neq 0}|c_m(t)|^2$. Given eq. (4), the latter formally recovers the expression given in [8], which captures the contribution to the density of excitations from states directly connected to $|\psi_0(t)\rangle$ via H_1 (see footnote [2]). Dynamical scaling emerges once the above result is supplemented by scaling assumptions on three fundamental dynamical variables: the time-dependent excitation energy above the ground state; the time-dependent matrix elements of the perturbation; and the density of excited states, $\rho(E)$, at the energy scale $\hat{t}^{-1}$ characterizing adiabaticity-breaking, which allows to change discrete sums over excited states to integrals. That is, close to the QCP we assume that

$$E_m(t) - E_0(t) = \delta\lambda(t)^{\nu z} f_m(\Delta_m(t_c)/\delta\lambda(t)^{\nu z}),$$
$$\langle\psi_m(t)|H_1|\psi_0(t)\rangle = \delta\lambda(t)^{\nu z - 1} g_m(\Delta_m(t_c)/\delta\lambda(t)^{\nu z}),$$
$$\rho(E) \sim E^{d/z - 1}, \qquad (5)$$

where the scaling functions f_m, g_m satisfy i) f_m (g_m) is constant when $x \to 0$; ii) f_m (g_m) $\propto x$ when $x \to \infty$ (see footnote [3]). Having the scaling assumptions at hand, integration over excited states is performed by moving to dimensionless variables $\zeta = (t - t_c)/\hat{t} = (t - t_c)\tau^{-\nu z/(\nu z + 1)}$ and $\eta = \Delta_m(t_c)\hat{t} = \Delta_m(t_c)\tau^{\nu z/(\nu z + 1)}$. Since at the QCP the integrand in eq. (4) develops a simple pole, while the phase $e^{i\int_{t_{\text{in}}}^{t'}\mathrm{d}s\,\Delta_m(s)}$ becomes stationary, contributions away from the QCP may be neglected, allowing the desired scaling factor to be isolated, up to a regular function depending only on ζ. Thus, the scaling of the excitation density and *diagonal observables* such as the residual energy is directly determined as $n_{\text{ex}}(\zeta) = \tau^{-d\nu/(\nu z + 1)}\Xi(\zeta)$, $\Delta H(\zeta) = \tau^{-(d+z)\nu/(\nu z + 1)}\Upsilon(\zeta)$, see also fig. 2. For a *generic observable*, if the additional scaling condition

$$\langle\psi_0(t)|\,\mathcal{O}\,|\psi_m(t)\rangle = \delta\lambda(t)^\beta q_m(\Delta_m(t_c)/\delta\lambda(t)^{\nu z}), \qquad (6)$$

holds for all the excitations m involved in the process for an appropriate scaling function q_m, then $\Delta\mathcal{O} \sim \tau^{-(\nu d + \beta)/(\nu z + 1)}$ – consistent with eq. (3).

Two remarks are in order. First, the above argument directly explains the dynamical scaling reported in [19] for generalized entanglement relative to the fermionic algebra $u(N)$ [23], whose ground-state equilibrium behavior directly reflects the fluctuations of the total number operator. Second, the derivation naturally extends to a generic non-linear *power law* quench, that is, $\delta\lambda(t) = \lambda(t) - \lambda_c = |(t - t_c)/\tau|^\alpha \text{sign}(t - t_c)$, $\alpha > 0$. Provided that the typical time scale for adiabaticity breaking is redefined as $\hat{t}_\alpha \sim \tau^{\alpha\nu z/(1 + \alpha\nu z)}$, the same scaling assumptions in eqs. (5), (6) lead to dynamical scaling behavior of the form $n_{ex} \sim \tau^{-\alpha d\nu/(\alpha\nu z + 1)}$, and $\Delta\mathcal{O} \sim \tau^{-\alpha(d\nu + \beta)/(\alpha\nu z + 1)}$, throughout the whole time evolution[4].

Quenching along paths involving a finite number of critical modes. – A first situation which is beyond the standard KZS discussed thus far arises in quenches that force the system along a critical line, yet are dominated by a finite number of participating excitations. *Formally*, this makes it possible to obtain the non-equilibrium exponent for n_{ex} through application of the KZS, provided care is taken in defining the static exponents through a limiting path-dependent process where, along the quench of interest, a *simultaneous* expansion with respect to both the control parameter *and* the relevant critical mode(s) is taken. Consider a quenching scheme where both h and δ are changed according to t/τ while $\gamma = 0$ (path $F \to O \to G$ in fig. 1). While eq. (2) shows that the mode $k = \pi/2$ is critical throughout the process ($\Delta_{\pi/2}(t) = 0$, for all $t \in [t_{\text{in}}, t_{\text{fin}}]$ as $N \to \infty$), numerical data indicate that excitation sets in only when the point O is passed, see fig. 3. As remarked, the static critical exponents at O are $z = 1, \nu = 1$, which differ from the critical exponents ($z = 2, \nu = 1/2$) of all other critical points along this line. Indeed, the non-equilibrium exponent is solely determined by the static exponents of this QCP along the chosen path, $n_{\text{ex}} \sim \tau^{-\nu/(\nu z + 1)} = \tau^{-1/2}$. We term a QCP which belongs to a different universality class than all other critical points along a critical line and sets the non-ergodic scaling a *dominant critical point for that line*[5]. Physically, although $\Delta_{\pi/2}$ closes along the critical line in the thermodynamic limit, a level crossing which brings all bands together only occurs at O – still allowing the time-evolved state to adiabatically follow the snapshot ground state until then. The following independent confirmations may be invoked in support of the above argument. First, consider the anisotropic quench process analyzed in [18], whereby $\gamma(t)$ is changed linearly along the critical line $h^2 = \delta^2 + 1$. By Taylor-expanding Δ_k in eq. (2) around $k = 0, \gamma = 0$

---

[2]In particular, since one-body perturbations H_1 are considered in the present analysis, the first-order excitation probability, $\mathbb{P}_{\text{ex}}^{(1)}(t) = \sum_{m\neq 0}|c_m^{(1)}(t)|^2$, coincides with the single-mode quasiparticle contribution, $\langle N_{k,n}\rangle = 1$, to the total time-dependent excitation density.

[3]Note that $\rho \sim \xi^{-d}/E$, with $\xi^d \sim \xi^m\xi^{d-m} \sim E^{-m/z}L^{d-m}$ for a $(d - m)$-dimensional critical surface.

[4]The perturbative derivation as presented strictly applies to quenches across an isolated QCP which is *not* multi-critical. We defer application of the perturbative derivation to a multi-critical point to a forthcoming analysis.

[5]The point O is multi-critical. However, quenches across a multi-critical point need *not* satisfy KZS, see [13].
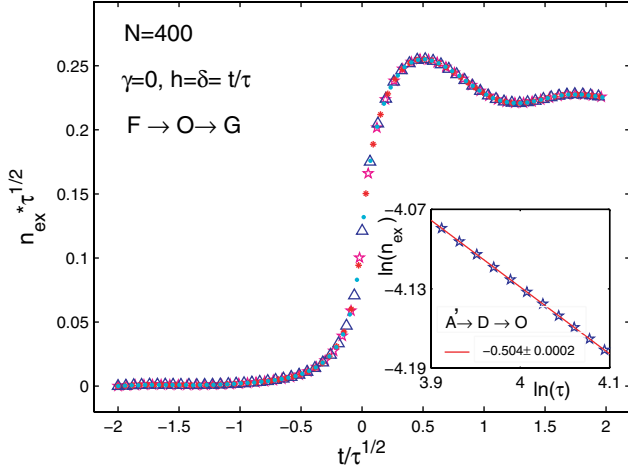
Fig. 3: (Colour on-line) Main panel: dynamical scaling of the excitation density for a simultaneous linear quench of h and δ along the gapless critical line $h = \delta$ ($F \to O \to G$). Inset: log-log plot of the final excitation density vs. τ along the path $A' \to D \to O$.

reveals that $\nu = 1, z = 2$ at the dominant QCP ($\gamma = 0, h, \delta$), whereas $\nu = 1, z = 1$ for $\gamma \neq 0$ along the line. Accordingly, $n_{\mathrm{ex}} \sim \tau^{-1/3}$. While this coincides with the result obtained in [18], the underlying physical explanation is different. Plots of the rescaled excitation density ($n_{\mathrm{ex}}\tau^{1/3}$) vs. the rescaled time ($t/\tau^{2/3}$) would collapse onto one another for different τ within the appropriate range, in complete analogy with fig. 3. Second, loss of adiabaticity at a single point can also explain the scaling behavior observed for an AFM-to-FM quench (or a critical-to-FM quench) in the XXZ model [16], whereby the control path involves the gapless critical region $-1 \leqslant \Delta \leqslant 1$ and the dominant critical point $\Delta = 1$ belongs to a different universality class. Lastly, the concept of a dominant QCP remains useful for a power law quench, which leads to the scaling behavior $n_{ex} \sim \tau^{-\alpha d\nu/(\alpha\nu z+1)}$, with ν and z being the critical exponents of the dominant QCP along the critical line.

Quenching along paths involving an infinite number of critical modes. – More complex scenarios emerge when uncountably many modes of excitations can compete during the quench. Focusing on the isotropic limit $\gamma = 0$, we contrast two representative situations where the Lifshitz QPT is involved: I) magnetic quenches along the path $D \to O \to E$ (PM $\to$ SF $\to$ PM); II) alternating quenches along the path $A \to B \to C$ (DM $\to$ SF $\to$ DM). Since $[M_z, H] = 0$, in both cases the allowed excitation must comply with a non-trivial dynamical constraint. Along the path $D \to O \to E$, this forces the final state to be the same as the initial ground state up to a global phase factor, leading to $n_{\mathrm{ex}}(t_{\mathrm{fin}}) \sim \tau^0$. Although for a magnetic quench this may be viewed as a consequence of the fact that the dynamics simply acts as a relabeling of the snapshot eigenstates, the same scaling holds for any quench which begins or ends in the gapless phase – for instance, a δ-quench along the path $A \to B$. Because

these quenches take the system through a critical line in momentum space, $d - m = 1$ (as opposed to $d - m = 0$ for an isolated QCP), the observed scaling is consistent with the recent prediction $n_{\mathrm{ex}}(t_{\mathrm{fin}}) \sim \tau^{-m\nu/(\nu z+1)}$ [15].

One may naively expect the same scaling to hold for path II), which also connects two gapped phases, albeit different than in I). Unlike in the standard KZS, however, details about the initial and final phases as well as the time-dependent excitation pattern become important. Specifically, along path II) we find $n_{\mathrm{ex}}(t_{\mathrm{fin}}) \sim \tau^{-1/2}$. An explanation may be obtained by exploiting the fact that, due to $U(1)$-symmetry, the fermion number is conserved. This allows the reduced 4×4 matrix H_k to be decoupled into two 2×2 matrices by interchanging the order of the basis vectors a_{-k} and $b_k^\dagger$. Thus, $\hat{H}_{\pm k} = W_{\pm k}^\dagger H'_{\pm k} W_{\pm k}$, where $W_k^\dagger = (a_k^\dagger, b_k^\dagger)$, $W_{-k}^\dagger = (a_{-k}, b_{-k})$, and

$$H'_{\pm k} = \pm 2h\mathbb{I}_2 + \begin{pmatrix} \pm 2\delta & \mp 2\cos k \\ \mp 2\cos k & \mp 2\delta \end{pmatrix}. \qquad (7)$$

For such a two-level system, the asymptotic excitation probability may be computed from the Landau-Zener transition formula [24], yielding $p_k = e^{-2\pi\cos^2 k\tau}$. Upon integrating over all modes, we find

$$n_{\mathrm{ex}}(t_{\mathrm{fin}}) = \frac{1}{\pi} \int_{-\pi/2}^{\pi/2} \mathrm{d}k \, p_k \sim \tau^{-1/2}. \qquad (8)$$

Note that because p_k is independent of h, the result in eq. (8) may be interpreted as implying that traversing the gapless phase produces the same excitation density as crossing the single QCP O by translating path II) at $h = 0$, which determines the non-equilibrium exponent.

Physical insight into what may be responsible for the different behavior observed in the two quenches is gained by looking at the excitation spectrum along the two paths. Notice that, once the energy eigenvalues are specified at the initial time, ($\epsilon_{k,1}(t_{\mathrm{in}}) \leqslant \epsilon_{k,2}(t_{\mathrm{in}}) \leqslant \epsilon_{k,3}(t_{\mathrm{in}}) \leqslant \epsilon_{k,4}(t_{\mathrm{in}})$ in our case), the same relative ordering need not hold at the final time if a level crossing is encountered during the quench – see fig. 4(a), (b). In the critical region, a pair of modes (k, n) and (k, n') undergoes a level crossing if $h^2 - \delta^2 = \cos^2 k$. If the number of such level crossings for fixed n, n' is even, the net contribution to the final excitation from momentum k is zero, since the final occupied bands are the same as the initial ones – see fig. 4(c). No cancellation is in place if either an odd number of level crossings from the same pair or if different pairs (n, n') are involved. The latter situation is realized for all k along path I) (h-quench, fig. 4(a)) and also for the path $A \to B$ (δ-quench). For a δ-quench along path II), the net excitation from the gapless phase turns out to be completely canceled (as seen in fig. 4(d), where the quench starts and ends symmetrically within the gapless phase). This only leaves the two boundary critical lines $h = \pm\delta$ as contributing to the excitation, thus a finite set of critical modes (a single one in fact, $k = \pi/2$, see fig. 4(b)).

Interestingly, a similar *cancellation mechanism* was verified for repeated quenches across an isolated QCP [11].
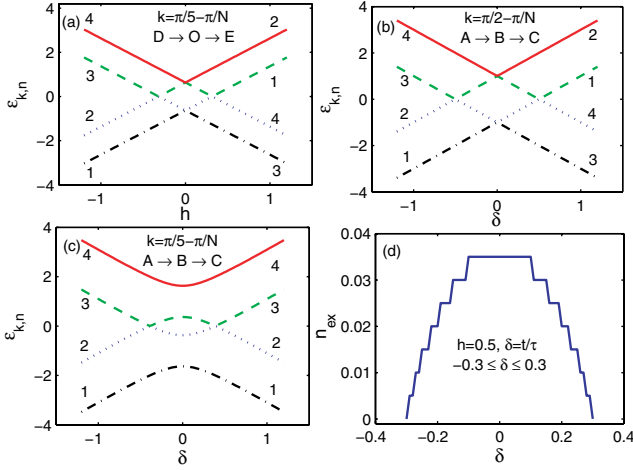
Fig. 4: (Colour on-line) Panels (a)–(c): band structure for different momentum modes k *vs.* quench parameter (*i.e.*, h or δ). Band ordering is determined by band index $n = 1, 2, 3, 4$ at initial time $t = t_{\text{in}}$, whereas dash-dotted (black) $\leqslant$ dotted (blue) $\leqslant$ dashed (green) $\leqslant$ solid (red) at a generic time t along the control path. Panel (d): final excitation density, $n_{\text{ex}}(t_{\text{fin}})$, *vs.* δ for a quench of the alternation strength δ at fixed $h = 0.5$ within the critical region. For all cases, $N = 400$.

While a thorough analysis is beyond our current scope, we suggest that even participation from the same (pair of) snapshot excitations may be at the root of this cancellation in both scenarios. Here, we further test this conjecture by examining the path $A' \to D \to O$, for which an effective two-level LZ mapping is no longer possible. Unlike $A \to B \to C$, two intermediate phases are now crossed, and the initial and final phase differ from one another, yet analysis of $\epsilon_{k,n}(t)$ reveals that the two paths are equivalent in terms of participation of critical modes. Numerical results confirm that $n_{\text{ex}}(t_{\text{fin}}) \sim \tau^{-1/2}$, fig. 3.

Conclusions. – Non-ergodic dynamical scaling is fully captured by first-order adiabatic renormalization for sufficiently slow quenches involving a simple isolated QCP. Beyond this regime, we find that non-equilibrium exponents remain expressible by combinations of equilibrium (path-dependent) ones in all the scenarios under examination, however a detailed characterization of both the static phase diagram and the accessible low-lying excitations is necessary for quantitative predictions. Ultimately, scaling behavior appears to be the same for control paths which share an equivalent excitation structure. While yet different non-ergodic scaling may arise in more complex systems (*e.g.*, infinite-order Berezinskii-Kosterlitz-Thouless QPTs [16] as well as models with infinite coordination [25]), a deeper analysis of how competing many-body excitations contribute and interfere during a quench may shed further light on non-equilibrium quantum critical physics.

$* * *$

REFERENCES

[1] Sachdev S., *Quantum Phase Transitions* (Cambridge University Press, Cambridge) 1999.
[2] Barouch E., McCoy B. M. and Dresden M., *Phys. Rev. A*, **2** (1970) 1075.
[3] Vallespir J. B., arXiv:quant-ph/0603124; Sen(De) A., Sen U. and Lewenstein M., *Phys. Rev. A*, **70** (2004) 060304.
[4] Zurek W. H., Dorner U. and Zoller P., *Phys. Rev. Lett.*, **95** (2005) 105701.
[5] Greiner M. *et al.*, *Nature*, **415** (2002) 39; Micheli A., Brennen G. K. and Zoller P., *Nat. Phys.*, **2** (2006) 341; Sadler L. E. *et al.*, *Nature*, **443** (2006) 312; Xu G. *et al.*, *Science*, **24** (2007) 317; Kummamuru R. K. and Soh Y.-A., *Nature*, **452** (2008) 859.
[6] Dziarmaga J., *Phys. Rev. Lett.*, **95** (2005) 245701; Damski B., *Phys. Rev. Lett.*, **95** (2005) 035701; Damski B. and Zurek W. H., *Phys. Rev. A*, **73** (2006) 063405; Cucchietti F. M. *et al.*, *Phys. Rev. A*, **75** (2007) 023603.
[7] Cherng R. W. and Levitov L. S., *Phys. Rev. A*, **73** (2006) 043614.
[8] Polkovnikov A., *Phys. Rev. B*, **72** (2005) 161201; Polkovnikov A. and Gritsev V., *Nat. Phys.*, **4** (2008) 477.
[9] Mondal S., Sen D. and Sengupta K., *Phys. Rev. B*, **78** (2008) 045101.
[10] Fubini A., Falci G. and Osterloh A., *New J. Phys.*, **9** (2007) 134.
[11] Mukherjee V., Dutta A. and Sen D., *Phys. Rev. B*, **77** (2008) 214427.
[12] Sen D., Sengupta K. and Mondal S., *Phys. Rev. Lett.*, **101** (2008) 016806; Barankov R. and Polkovnikov A., *Phys. Rev. Lett.*, **101** (2008) 076801.
[13] Divakaran U., Mukherjee V., Dutta A. and Sen D., arXiv:0807.3606; Mondal S., Sengupta K. and Sen D., arXiv:0808.1175.
[14] Dziarmaga J., *Phys. Rev. B*, **74** (2006) 064416; Caneva T., Fazio R. and Santoro G. E., *Phys. Rev. B*, **76** (2007) 144427.
[15] Sengupta K., Sen D. and Mondal S., *Phys. Rev. Lett.*, **100** (2008) 077204.
[16] Pellegrini F. *et al.*, *Phys. Rev. B*, **77** (2008) 140404.
[17] Mukherjee V. *et al.*, *Phys. Rev. B*, **76** (2007) 174303.
[18] Divakaran U., Dutta A. and Sen D., *Phys. Rev. B*, **78** (2008) 144301.
[19] Deng S., Viola L. and Ortiz G., in *Recent Progress in Many-Body Theories*, Vol. **11** (World Scientific, Singapore) 2008, p. 387, arXiv:0802.3941.
[20] Berry M. V., *Proc. R. Soc. A*, **14** (1987) 31.
[21] Okamoto K. and Yasumura K., *J. Phys. Soc. Jpn.*, **59** (1990) 993; Derzhko O., Richter J., Krokhmalskii T. and Zaburannyi O., *Phys. Rev. E*, **69** (2004) 066112.
[22] Messiah A., *Quantum Mechanics* (North-Holland, Amsterdam) 1962, Chapt. XVII.
[23] Barnum H. *et al.*, *Phys. Rev. Lett.*, **92** (2004) 107902; Somma R. *et al.*, *Phys. Rev. A*, **70** (2004) 042311.
[24] Zener C., *Proc. R. Soc. London, Ser. A*, **137** (1932) 696.
[25] Caneva T., Fazio R. and Santoro G. E., arXiv:0806.4455.